Pergamon

Int. J. Heat Mass Transfer. Vol. 40, No. 13, pp. 3237–3245, 1997
© 1997 Elsevier Science Ltd. All rights reserved
Printed in Great Britain
0017-9310/97 $17.00+0.00

PII: S0017-9310(96)00215-3

Numerical analysis of InP solution growth by travelling heater method: transient response in the case of no heater movement

SATOSHI MATSUMOTO and TORU MAEKAWA†
Department of Mechanical Engineering, Toyo University, 2100, Kujirai, Kawagoe, Saitama 350, Japan

and

KATSUMI TAKAHASHI
Ishikawajima-Harima Heavy Industry, 3-1-15, Toyosu, Koto-ku, Tokyo 135, Japan

(*Received* 30 *November* 1995 *and in final form* 12 *April* 1996)

Abstract—We carried out a numerical simulation of InP solution growth by the travelling heater method (THM). We introduced the governing equations and made clear the parameters which govern solution growth by THM. The velocity, temperature and concentration fields and the solidification processes were simulated by the finite difference method and the boundary fit method. The effect of thermal convection on the crystal growth rate and the constitutional supercooling occurring in indium solvent was investigated.
© 1997 Elsevier Science Ltd.

INTRODUCTION

The travelling heater method (THM) is considered to be one hope for growing single high quality III–V or II–VI compound crystals which will be future materials for fast electronic or optical devices, and has been investigated experimentally [1–13]. A. N. Danilewsky *et al.* [6, 8, 9] were the first researchers to grow InP by the travelling heater method. They showed that it is difficult to grow a single long crystal by solution growth.

Although quite a few experiments have been carried out, there are not enough theoretical or numerical studies and it is necessary to do theoretical and numerical work in order to understand crystal growth by THM quantitatively. H. E. Sell and G. Müller [14] carried out a numerical modelling and a one-dimensional numerical simulation. Yu. V. Apanovich and E. D. Ljumkis [15] were the first researchers to carry out a two-dimensional analysis of solution growth by THM including the effect of thermal convection. S. Matsumoto *et al.* [16] carried out a numerical analysis of melt growth by THM using the boundary fit method and made clear the effect of thermal convection on the shape of the melt-crystal interface.

In the case of solution growth, the temperature and concentration at the solution–crystal interface and the shape of the solution–crystal interface are unknown and therefore must be determined by phase diagrams. Another important factor is constitutional supercooling which may occur in the solution and may, therefore, generate polycrystals. Our ultimate goal is to find the optimal conditions for obtaining single high quality compound crystals by THM and the purpose of our present study is, as a first step, to introduce a mathematical model for InP solution growth by THM, to solve the problem numerically and to make clear the effect of buoyancy convection on the supercooling occurring in the solution. In this paper, we focus on the transient crystal growth process with no heater movement until the process reaches the steady-state. We are also investigating the effect of heater speed, the result of which will be published soon.

In the first section, a mathematical model and the governing equations are introduced. In the next section, the numerical technique using the boundary fit method is explained so that the position and shape of the solution–crystal interface can be treated as unknown factors. In the final section, the result of the numerical simulation is shown and the effect of buoyancy convection on the growth rate and the constitutional supercooling is discussed.

MATHEMATICAL MODEL AND GOVERNING EQUATIONS

We made a model of crystal growth by THM as shown in Fig. 1. The calculation area is divided into three regions; (1) Solid I (single crystal rod); (2) Solution; (3) Solid II (feed rod). The solution and the

† Author to whom correspondence should be addressed.

NOMENCLATURE

A	aspect ratio (Fig. 1)
c	absolute concentration of phosphorus
C	concentration of phosphorus (equation (9))
c_p	specific heat at constant pressure
D	diffusion coefficient of phosphorus in indium solvent
F^*	nondimensional position of interface
g	gravitational acceleration
K	nondimensional number (equation (18))
L_{sl}	latent heat
Pr	Prandtl number (equation (18))
q	heat flux
q_0	heat flux (equation (1))
Q	nondimensional heat flux, q/q_0
r	r-coordinate
$\mathbf{r}$	position vector
r_0	radius of ampoule
R	nondimensional r-coordinate
Ra^C	Rayleigh number based on concentration (equation (18))
Ra^T	Rayleigh number based on temperature (equation (18))
S	degree of constitutional supercooling (equation (22))
Sc	Schmidt number (equation (18))
Sf	Stefan number (equation (18))
t	time
T	temperature
Ta	Taylor number (equation (18))
V	nondimensional velocity
z	z-coordinate
Z	non-dimensional z-coordinate
Z_0	position of centre of heater.

Greek symbols

β	temperature coefficient of volume expansion
γ	concentration coefficient of volume expansion
η	coordinate (equation (19))
θ	nondimensional temperature
κ	thermal diffusivity
λ	thermal conductivity
ν	kinematic viscosity
ξ_1	coordinate (equation (20))
ξ_2	coordinate (equation (21))
ρ_0	density
τ	nondimensional time
Ψ	nondimensional stream function
ω	nondimensional vorticity
Ω	angular frequency.

Subscripts

f	melting point of InP
L	solution
R	radial component
S1	solid I
S2	solid II
Z	vertical component
ϕ	angular component
1	interface between solution and solid I
2	interface between solution and solid II.

solids are placed in a vertical cylindrical ampoule. The solution has a free surface and is heated by a lateral heater. The heat flux at the surface is given externally as equation (1), which is based on our experimental system using a mirror furnace.

$$q = q_0 f(Z - Z_0)$$

$$f(Z) = aZ^8 + bZ^6 + cZ^4 + dZ^2 + e \qquad (1)$$

where Z is the nondimensional coordinate in the vertical direction (see Fig. 1) and $f(Z)$ is dimensionless. Coefficients a, b, c, d and e are dependent on the furnace and 2.48×10^{14}, -2.17×10^{11}, 7.29×10^{7}, -1.20×10^{4} and 1.0 are assigned in our case. q is the total heat flux including radiative and convective heat transfer at the surface and the temperature and heat flux will be nondimensionalised using q_0 later. The heat is removed from the top and the bottom. The heat input from the heater is equal to the amount of heat output removed from the top and the bottom. The lateral wall is thermally insulated except in the heated regions. The ampoule is rotated at an angular frequency of Ω. The temperature at the solution–solid interface and the concentration of phosphorus at the solution side of the interface are unknown and, therefore, must be determined by the liquidus curve of the InP phase diagram [17], which is shown in Fig. 2.

In this section, the nondimensional governing equations and the boundary conditions are introduced for each region and the parameters which govern crystal growth by THM are made clear. The coordinate $\mathbf{r}$ and time t are nondimensionalised as below:

$$\mathbf{R} \equiv \frac{\mathbf{r}}{r_0}, \quad \tau \equiv \Omega t. \qquad (2)$$

Solution

Momentum equations. Applying Boussinesq approximation, the momentum equations in the solution are expressed as below:

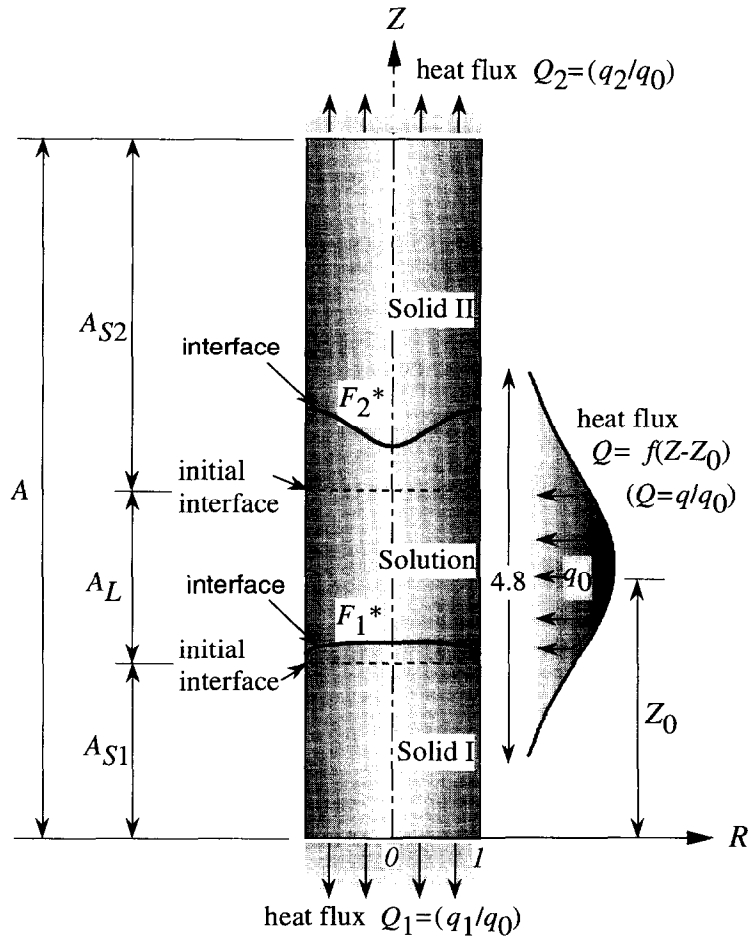

Fig. 1. Numerical model of crystal growth by THM.

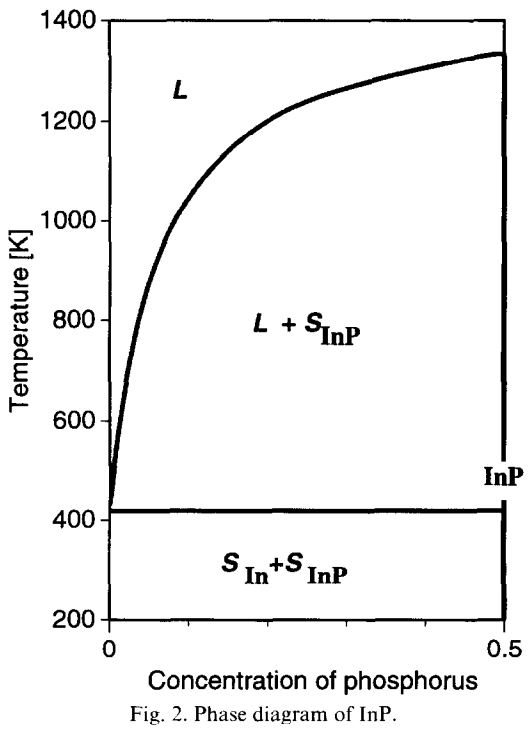

Fig. 2. Phase diagram of InP.

$$\frac{\partial\omega}{\partial\tau}+V_R\frac{\partial\omega}{\partial R}+V_Z\frac{\partial\omega}{\partial Z}-\frac{V_R\omega}{R}-\frac{1}{R}\frac{\partial V_\phi^2}{\partial Z}$$
$$=\frac{1}{Ta}\left[\frac{\partial^2\omega}{\partial R^2}+\frac{1}{R}\frac{\partial\omega}{\partial R}+\frac{\partial^2\omega}{\partial Z^2}-\frac{\omega}{R^2}\right]$$
$$-\frac{Ra^T}{Pr\cdot Ta^2}\frac{\partial\theta_L}{\partial R}-\frac{Ra^C}{Sc\cdot Ta^2}\frac{\partial C_L}{\partial R} \quad (3)$$

$$\frac{\partial V_\phi}{\partial\tau}+V_R\frac{\partial V_\phi}{\partial R}+V_Z\frac{\partial V_\phi}{\partial Z}+\frac{V_RV_\phi}{R}$$
$$=\frac{1}{Ta}\left[\frac{\partial^2V_\phi}{\partial R^2}+\frac{1}{R}\frac{\partial V_\phi}{\partial R}+\frac{\partial^2V_\phi}{\partial Z^2}-\frac{V_\phi}{R^2}\right] \quad (4)$$

where the velocity is nondimensionalised by $r_0\Omega$, and Ψ, V_ϕ and ω are the nondimensional stream function, circumferential velocity and vorticity, respectively.

$$V_R=\frac{1}{R}\frac{\partial\Psi}{\partial Z},\quad V_Z=-\frac{1}{R}\frac{\partial\Psi}{\partial R} \quad (5)$$

$$\omega\equiv\frac{\partial V_R}{\partial Z}-\frac{\partial V_Z}{\partial R}=\frac{1}{R}\frac{\partial^2\Psi}{\partial R^2}-\frac{1}{R^2}\frac{\partial\Psi}{\partial R}+\frac{1}{R}\frac{\partial^2\Psi}{\partial Z^2} \quad (6)$$

where V_R and V_Z are the velocity components in the radial and vertical directions, respectively.

Energy equations.

$$\frac{\partial\theta_L}{\partial\tau}+V_R\frac{\partial\theta_L}{\partial R}+V_Z\frac{\partial\theta_L}{\partial Z}=\frac{1}{Pr\cdot Ta}\left[\frac{\partial^2\theta_L}{\partial R^2}+\frac{1}{R}\frac{\partial\theta_L}{\partial R}+\frac{\partial^2\theta_L}{\partial Z^2}\right] \quad (7)$$

Transport equation of phosphorus.

$$\frac{\partial C_L}{\partial\tau}+V_R\frac{\partial C_L}{\partial R}+V_Z\frac{\partial C_L}{\partial Z}=\frac{1}{Sc\cdot Ta}\left[\frac{\partial^2 C_L}{\partial R^2}+\frac{1}{R}\frac{\partial C_L}{\partial R}+\frac{\partial^2 C_L}{\partial Z^2}\right] \quad (8)$$

θ_L and C_L are the nondimensional temperature and the nondimensional concentration of phosphorus in indium solvent.

$$\theta_L\equiv\frac{T_L-T_f}{q_0 r_0/\lambda_L},\quad C_L\equiv\frac{c_L-0.5}{\Delta c} \quad (9)$$

where c_L is the absolute concentration of phosphorus ($0\leqslant c_L\leqslant 0.5$) and Δc is the characteristic concentration difference, that is, -0.5, in the present case.

The boundary conditions are

$R=0$:

$$V_R=0,\ V_\phi=0,\quad \omega=0,\quad \Psi=0,\quad \frac{\partial\theta_L}{\partial R}=0,$$

$$\frac{\partial C_L}{\partial R}=0$$

$R=1$:

$$V_R=0,\quad \frac{\partial V_\phi}{\partial R}=0,\quad \omega=0,\quad \Psi=0,$$

$$\frac{\partial\theta_L}{\partial R}=f(Z-Z_0),\quad \frac{\partial C_L}{\partial R}=0$$

$Z=F_1^*$:

$$V_R=0,\quad V_Z=0,\quad V_\phi=R,\quad \omega=\frac{1}{R}\frac{\partial^2\Psi}{\partial Z^2},\quad \Psi=0$$

$Z=F_2^*$:

$$V_R=0,\quad V_Z=0,\quad V_\phi=R,\quad \omega=\frac{1}{R}\frac{\partial^2\Psi}{\partial Z^2},\quad \Psi=0 \quad (10)$$

where F_1^* and F_2^* are the positions of the interface nondimensionalised by r_0. We assume that $V_R=V_Z=0$ at $Z=F_1^*, F_2^*$ as $\partial F_1^*/\partial\tau$ and $\partial F_2^*/\partial\tau$ are very small.

Solids I *and* II

Heat conduction equation.

$$\frac{\partial\theta_{Si}}{\partial\tau}=\frac{K_{Si}}{Pr\cdot Ta}\left[\frac{\partial^2\theta_{Si}}{\partial R^2}+\frac{1}{R}\frac{\partial\theta_{Si}}{\partial R}+\frac{\partial^2\theta_{Si}}{\partial Z^2}\right] \quad (11)$$

where i $(=1,2)$ corresponds to solid I and solid II, respectively. θ_{Si} is the nondimensional temperature of solids I and II.

$$\theta_{Si}\equiv\frac{T_{Si}-T_f}{q_0 r_0/\lambda_{Si}} \quad (12)$$

where T_f is the melting temperature of InP.

As the concentration of phosphorus is 0.5 in solid I and solid II, the diffusion equation does not need to be solved. In this case, C_{Si} $[\equiv(c_{Si}-0.5)/\Delta c)]=0$.

The boundary conditions are

$$R=0:\quad \frac{\partial\theta_{Si}}{\partial R}=0$$

$$R=1:\quad \begin{cases}\dfrac{\partial\theta_{Si}}{\partial R}=0 & \text{(nonheated surface)}\\ \dfrac{\partial\theta_{Si}}{\partial R}=f(Z-Z_0) & \text{(heated surface)}\end{cases}$$

$$Z=0:\quad \frac{\partial\theta_{S1}}{\partial Z}=Q_1$$

$$Z=A:\quad \frac{\partial\theta_{S2}}{\partial Z}=-Q_2 \quad (13)$$

Heat and mass balance between solid and solution

The heat and mass are balanced at the solution–solid interface [18] and the balance equations are expressed as below.

$$\frac{\partial F_i^*}{\partial\tau}=-\frac{Sf_L}{Pr\cdot Ta}\left\{\left[-\frac{\partial F_i^*}{\partial R}\frac{\partial\theta_L}{\partial R}+\frac{\partial\theta_L}{\partial Z}\right]-\left[-\frac{\partial F_i^*}{\partial R}\frac{\partial\theta_{Si}}{\partial R}+\frac{\partial\theta_{Si}}{\partial Z}\right]\right\} \quad (14)$$

$$(C_L-C_{Si})\frac{\partial F_i^*}{\partial\tau}=-\frac{1}{Sc\cdot Ta}\left[-\frac{\partial F_i^*}{\partial R}\frac{\partial C_L}{\partial R}+\frac{\partial C_L}{\partial Z}\right] \quad (15)$$

where F_i^* $(i=1,2)$ corresponds to the solution–solid I and solution–solid II interfaces. In fact, $C_{Si}=0$ according to our definition of the concentration (equation (9)).

As $(\partial\theta_L/\partial R)_{Z=F^*,R=1}=(\partial\theta_S/\partial R)_{Z=F^*,R=1}$, the boundary conditions for F_i^* are introduced as below

$$R=0:\quad \frac{\partial F_i^*}{\partial R}=0,\quad R=1:\quad \frac{\partial F_i^*}{\partial R}=0 \quad (16)$$

In equations (14) and (15), the temperature and the concentration at the solution–solid interface are related by the liquidus curve which is shown in Fig. 2 [17]. We approximated the curve as below:

$$\begin{aligned}c_L=&-9.148\times10^{-23}T^8+6.578\times10^{-19}T^7\\&-2.018\times10^{-15}T^6+3.454\times10^{-12}T^5\\&-3.606\times10^{-9}T^4+2.351\times10^{-6}T^3\\&-9.354\times10^{-4}T^2+2.076\times10^{-1}T-1.970\end{aligned} \quad (17)$$

The nondimensional parameters which appeared in the governing equations are summarized below.

$$Ra^{T} \equiv \frac{\beta \cdot g \cdot q_0 \cdot r_0^4}{\lambda_L \cdot \kappa_L \cdot \nu_L}, \quad Ra^{C} \equiv \frac{\gamma \cdot g \cdot \Delta c \cdot r_0^3}{D_L \cdot \nu_L},$$

$$Ta = \frac{r_0^2 \cdot \Omega}{\nu_L}, \quad Pr \equiv \frac{\nu_L}{\kappa_L}, \quad Sc \equiv \frac{\nu_L}{D_L},$$

$$K_{Si} \equiv \frac{\kappa_{Si}}{\kappa_L}, \quad Sf_L = \frac{q_0 \cdot r_0 \cdot C_{pL}}{L_{sl} \cdot \lambda_L} \tag{18}$$

NUMERICAL TECHNIQUE

The shapes of the solution–solid interface F_1^* and F_2^* change in time. Therefore, we solved the problem by the boundary fit method. The equations are transformed into more convenient forms by the coordinate transformations shown in equations (19), (20) and (21):

$$\eta \equiv \frac{Z - F_1^*}{F_2^* - F_1^*} \quad \text{(solution)} \tag{19}$$

$$\xi_1 \equiv \frac{Z}{F_1^*} \quad \text{(solid I)} \tag{20}$$

$$\xi_2 \equiv \frac{Z - F_2^*}{A - F_2^*} \quad \text{(Solid II)} \tag{21}$$

The transformed governing equations were solved under the boundary conditions by the finite difference method. We carried out simulations changing the number of grid points: 11 (radial direction) × 33 (vertical direction), 21 × 83 and 31 × 123. The maximum difference in the values of the streamfunction, temperature, concentration and position of the interface was within 3.2%. The Prandtl number and Schmidt number were, respectively, 7×10^{-3} and 3.7 which were estimated by the physical properties of InP [6] and the Taylor number was fixed at 150, which corresponds to 5 rpm if the radius of the ampoule is 5 mm. The initial aspect ratios of solution, solid I and solid II were, respectively, 2, 2 and 4. The initial temperature of the system was set at the melting point of indium and the initial concentration of phosphorus in the indium solvent was zero. The ratio of the heat flux q_1/q_2 was 2. The Rayleigh number was also estimated by the physical properties in ref. [6]. The Rayleigh number based on the temperature difference, Ra^{T}, was changed: 0, 10, 10^2, 10^3. The Rayleigh number based on the concentration difference, Ra^{C}, was 5×10^5.

RESULT OF NUMERICAL ANALYSIS AND DISCUSSION

We investigated the transient crystal growth process with a heater speed of zero until the system reached the steady state. The time variation of the position of the solution–solid I interface at the centre is shown in

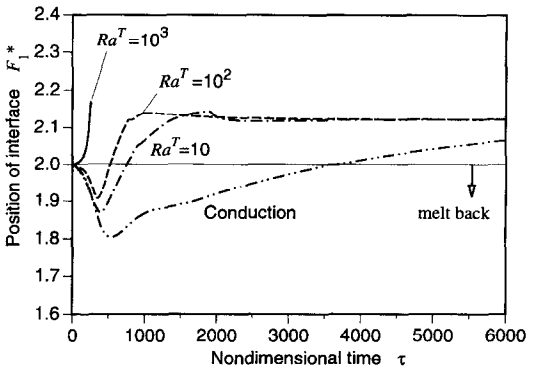

Fig. 3. Time variation of solution–solid I interface.

Fig. 3, where the initial position of the interface is located at $Z = 2$ and the interface movement in a pure conduction case is also shown for comparison. In the case of buoyancy convection for $Ra^{T} = 10$ and $Ra^{T} = 10^2$, noticeable melt-back occurs and crystal starts growing after a positive phosphorus concentration gradient has been established at the solution-crystal interface. In the case of strong buoyancy convection ($Ra^{T} = 10^3$), although meltback occurs in the early stage, the negative phosphorus concentration gradient is not very high and a positive phosphorus gradient is established very quickly.

The streamlines, isotherms, isoconcentration lines and solution–solid interfaces are shown in Fig. 4. Note that the nondimensional temperature is negative when the temperature is lower than the melting point (see the definition of the nondimensional temperature, equations (9) and (12)) and that the absolute concentration of phosphorus is indicated in the figure (see equation (9)). Although the Rayleigh number based on the concentration is larger than that based on the temperature, buoyancy convection driven by the concentration gradient is not strong even compared to convection induced by rotation according to our calculation because the Schmidt number is much larger than the Prandtl number and the concentration gradient is not very large. Especially, the effect of buoyancy convection driven by the concentration difference disappears in the steady state since the concentration gradient becomes zero. In the case of $Ra^{T} = 10$ (Fig. 4(a)), a small cell remains in the upper part of the solution which is induced by rotation, while thermal convection becomes dominant in the case of $Ra^{T} = 10^2$ and 10^3 (Fig. 4(b), (c)). In the case of buoyancy convection of $Ra^{T} = 10$ and 10^2, the concentration of phosphorus becomes minimal in the central part of the solution in the early stages, which explains why melt-back occurs. The temperature at the interface is lower than the melting point of InP and the process reaches its steady state when the concentration of phosphorus becomes uniform in the solution. In the case of strong buoyancy convection ($Ra^{T} = 10^3$), a positive phosphorus gradient is established very quickly at the interface.

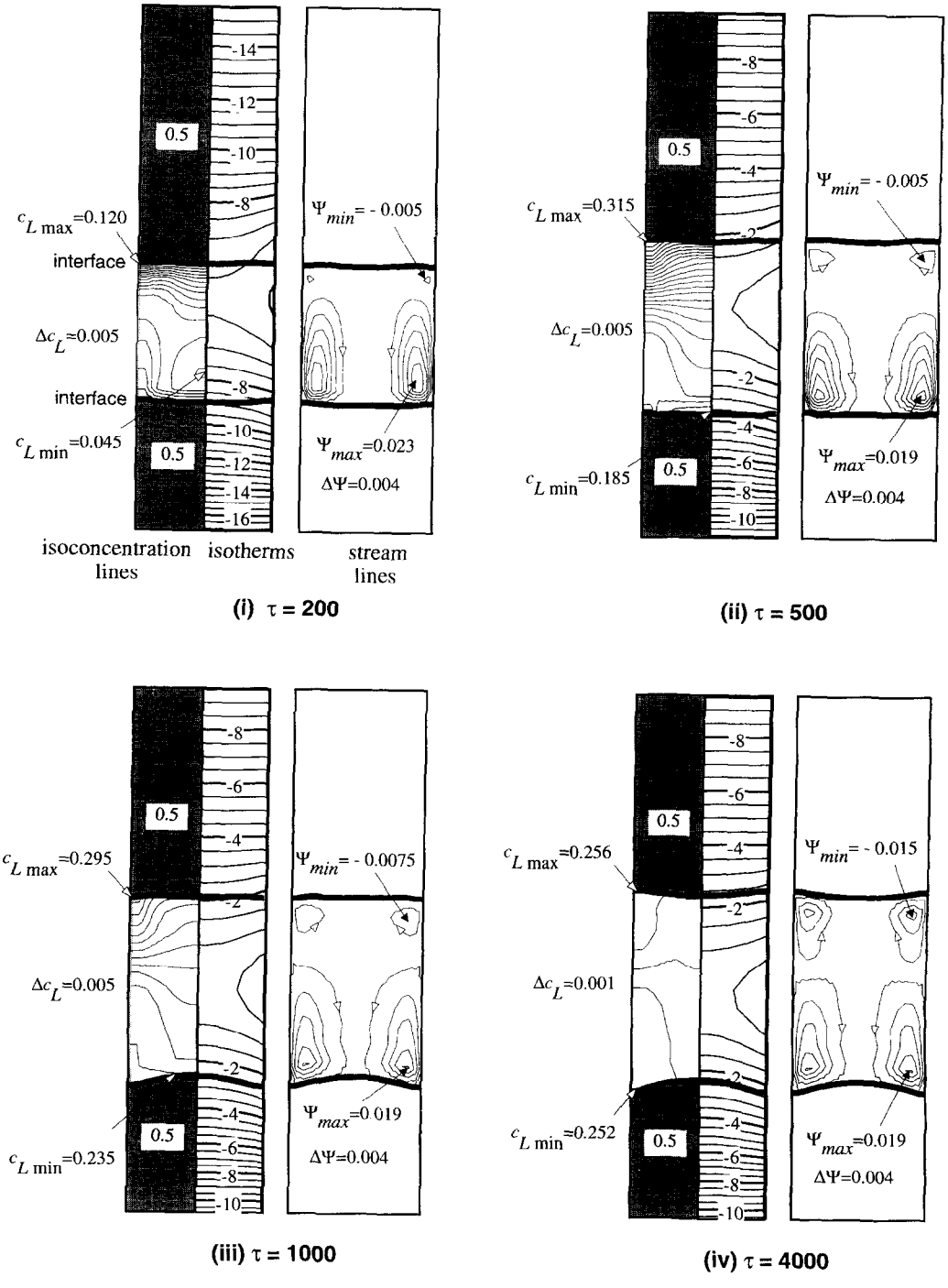

(a) Ra^T=10, Ra^C=5×10^5, Ta=150

Fig. 4. Streamlines, isotherms, isoconcentration lines and interface shape: (a) $Ra^T = 10$, $Ra^C = 5 \times 10^5$, $Ta = 150$; (b) $Ra^T = 10^2$, $Ra^C = 5 \times 10^5$, $Ta = 150$; (c) $Ra^T = 10^3$, $Ra^C = 5 \times 10^5$, $Ta = 150$. (*Continued opposite and overleaf.*)

One of the most important factors in solution growth is constitutional supercooling. Polycrystals may be produced if an area is supercooled. The region where the calculated concentration is higher than the saturation concentration corresponding to the calculated local temperature is supersaturated or supercooled. We defined the degree of the constitutional supercooling as below.

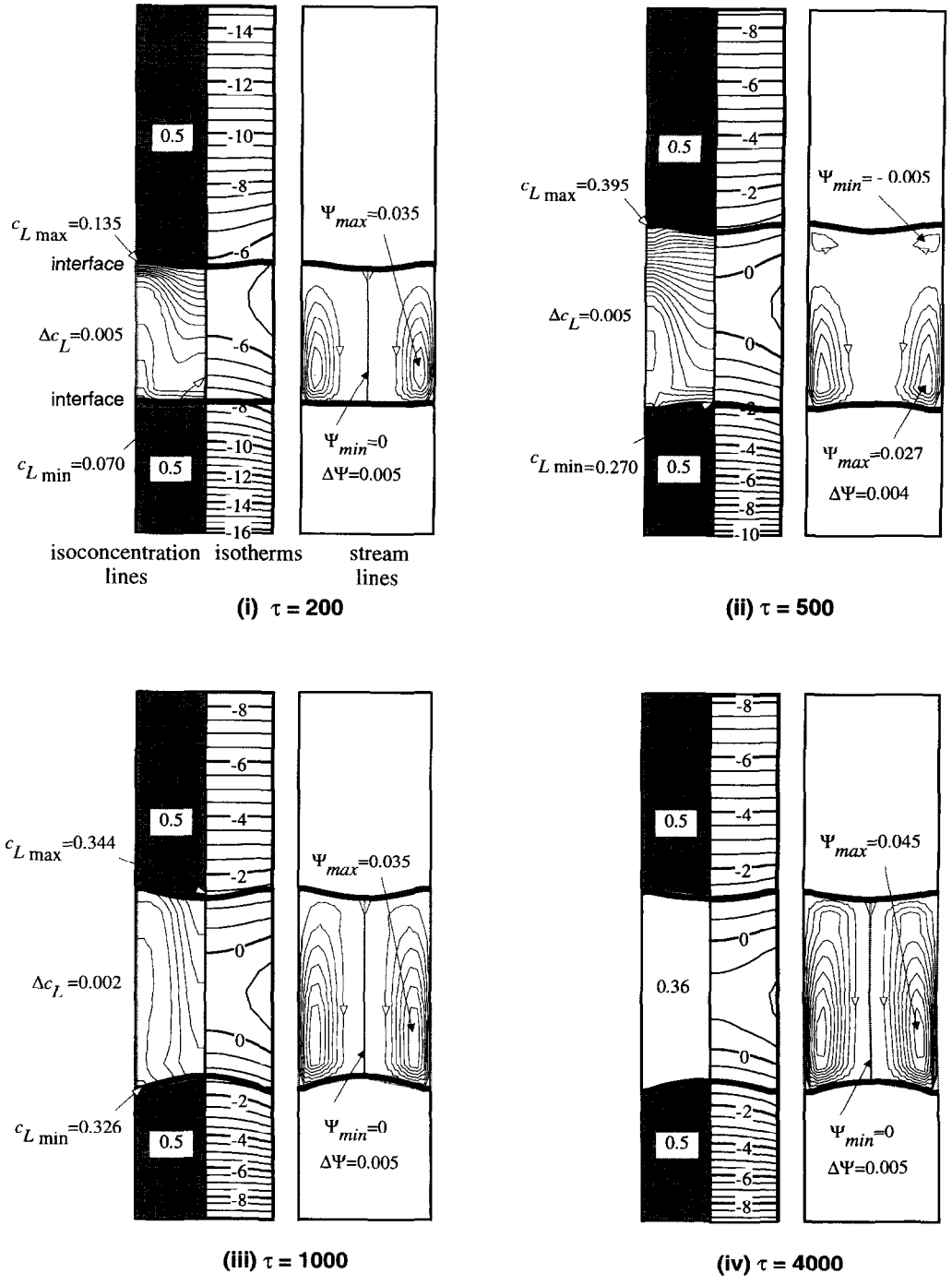

(b) $Ra^T=10^2$, $Ra^C=5\times10^5$, Ta=150

Fig. 4—*Continued.*

$$S \equiv \frac{c - c_{sat}}{c_{sat}} \tag{22}$$

where c_{sat} is the saturation concentration of phosphorus in the indium solvent corresponding to the local temperature. The area where S is positive is supercooled. In our calculation, constitutional supercooling occurred only in the case of $Ra^T = 10^3$. The time variation of the supercooled area is illustrated in Fig. 5. Strong supercooling occurs near the solution-

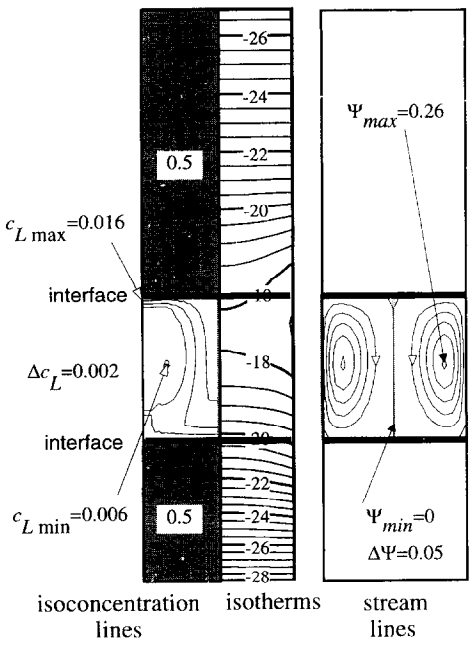

(i) τ =10

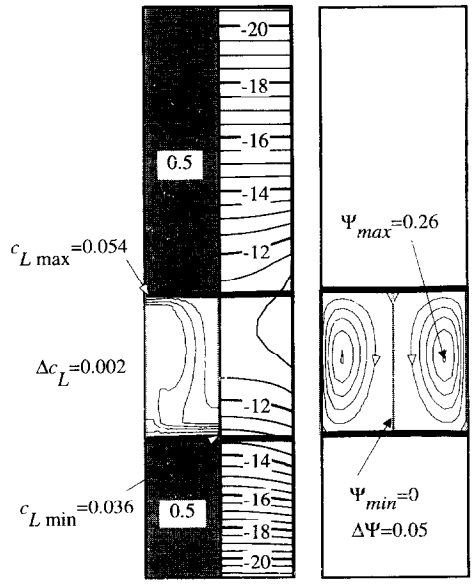

(ii) τ =100

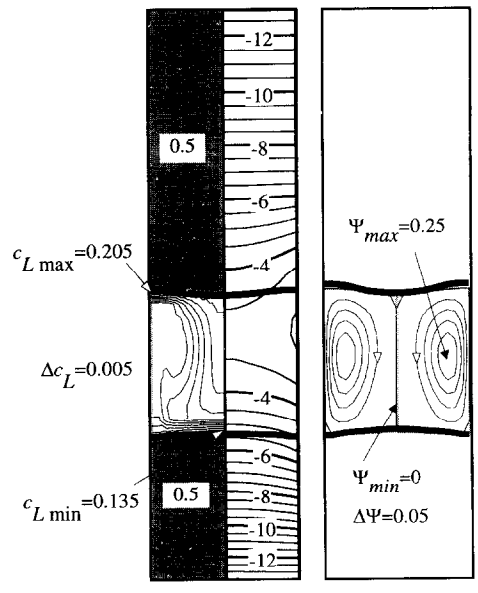

(iii) τ = 200

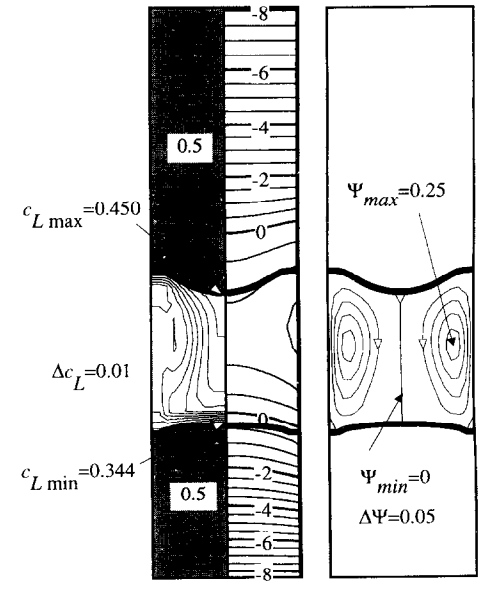

(iv) τ = 250

(c) Ra^T =10^3, Ra^C=5×10^5, Ta=150

Fig. 4—*Continued.*

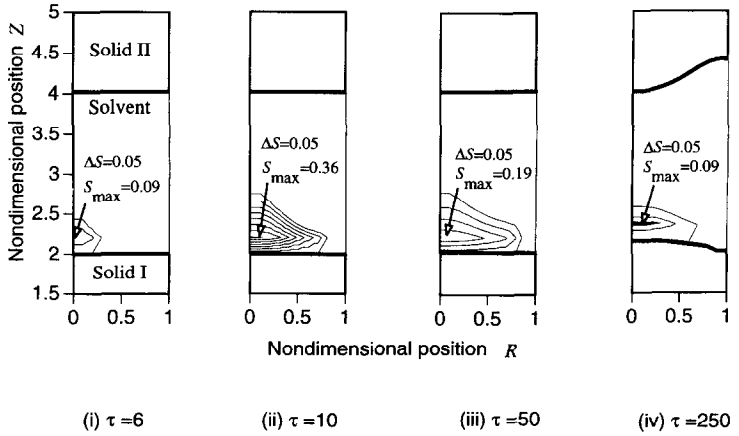

Fig. 5. Constitutional supercooled region ($Ra^T = 10^3$, $Ra^C = 5 \times 10^5$, $Ta = 150$).

crystal interface in the early stage. InP crystal growth may be affected by this strong supercooling [6, 8].

CONCLUSION

We studied InP solution growth by THM numerically. The transient crystal growth process was simulated without heater movement until the process reached a steady state. The calculation was successfully carried out by the boundary fit method and the finite difference method. It has been found that constitutional supercooling tends to occur near the interface in the case of strong buoyancy convection, while it does not appear in the case of weak buoyancy convection.

Acknowledgements—This study has been supported by the Grant-in-Aid for Scientific Research on Priority Areas of the Ministry of Education, Science and Culture, Japan.

REFERENCES

1. Rudolph, P., Engel, A., Schentke, I. and Grochocki, A., Distribution and genesis of inclusions in CdTe and (Cd, Zn) Te single crystals grown by the Bridgman method and by the travelling heater method. *Journal of Crystal Growth*, 1995, **147,** 297–304.
2. Triboulet, R., The travelling heater method (THM) for the $Hg_{1-x}Cd_xTe$ and related materials. *Progressive Crystal Growth Characteristic Matter*, 1994, **28,** 85–144.
3. Weiss, E., Kedar, E. and Mainzer, N., The formation of twins in ⟨111⟩ HgCdTe grown by travelling heater method and their effect on device quality. *Journal of Crystal Growth*, 1993, **132,** 191–199.
4. Baldus, A. and Benz, K. W., Melt and metallic solution crystal growth of $CuInSe_2$. *Journal of Crystal Growth*, 1993, **130,** 37–44.
5. Shoji, T., Hiratate, Y. and Onabe, H., Evaluation of CdTe(Cl) crystal growth with THM and application to a multichannel detector. *Nuclear Instrumental Methods in the Physics Research Section A*, 1992, **322,** 324–330.
6. Danilewsky, A. N., Dold, P. and Benz, K. W., The influence of axial magnetic fields on the growth of III–V semiconductors from metallic solutions. *Journal of Crystal Growth*, 1992, **121,** 305–314.
7. Assenov, R. and Polychroniadis, E. K., On the comparative characterization of single crystalline PbTe(I) grown by vertical Bridgman and travelling heater methods. *Journal of Crystal Growth*, 1991, **112,** 227–234.
8. Danilewsky, A. N., Benz, K. W. and Nishinaga, T., Growth kinetics in space- and earth-grown InP and GaSb crystals. *Journal of Crystal Growth*, 1990, **99,** 1281–1286.
9. Danilewsky, A. N. and Benz, K. W., InP growth from In solutions under reduced gravity. *Journal of Crystal Growth*, 1989, **97,** 571–577.
10. Bischopink, G. and Benz, K. W., THM growth and properties of $In_{1-x}Ga_xP$ bulk material. *Journal of Crystal Growth*, 1989, **97,** 245–253.
11. Tenne, R., Brener, R. and Triboulet, R., Chemical modifications of $Hg_{0.1}Cd_{0.9}Te$ surfaces: analysis with Auger electron spectroscopy. *Journal of Vacuum Science Technology A*, 1989, **7,** 2570–2574.
12. Colombo, L., Chang, R. R., Chang, C. J. and Baird, B. A., Growth of Hg-based alloys by the travelling heater method. *Journal of Vacuum Science Technology A*, 1988, **6,** 2795–2799.
13. Kim, K. M., Hahn, S. R., Noh, S. K., Park, H. L. and Chung, C. H., Temperature dependence of the Hall effect of THM-grown $Hg_{1-x}Cd_xTe$ crystals. *Journal of Crystal Growth*, 1988, **86,** 673–676.
14. Sell, H. E. and Müller, G., Numerical modelling of the growth and composition of $Ga_xIn_{1-x}As$ bulk mixed crystals by the travelling heater method. *Journal of Crystal Growth*, 1989, **97,** 194–200.
15. Apanvich, Yu. V. and Ljumkis, E. D., The numerical simulation of heat and mass transfer during growth of a binary system by the travelling heater method. *Journal of Crystal Growth*, 1991, **110,** 839–854.
16. Matsumoto, S., Maekawa, T., Takahashi, K. and Adachi, S., Numerical simulation of crystal growth by travelling heater method. *Proceedings of the ASME/JSME Thermal Engineering Joint Conference*, 1995, **4,** 61–69.
17. van den Boomgaard, J. and Schol, K., The P-T-x phase diagrams of the systems In-As, Ga-As and In-P. *Philips Research Report*, 1957, **12,** 127–140.
18. Meyer, G. H., A numerical method for the solidification of a binary alloy. *International Journal of Heat & Mass Transfer*, 1981, **24,** 778–781.